This is to certify that the

thesis entitled

RECRYSTALLIZATION KINETICS, MICROSTRUCTURE, AND TEXTURE DEVELOPMENT IN BORON DOPED NI_3AL

presented by

Pavan Nagpal

has been accepted towards fulfillment
of the requirements for

M.S. degree in Materials Science

Dr. G. Gottstein
Major professor

Date May 22, 1987

RECRYSTALLIZATION KINETICS, MICROSTRUCTURE AND TEXTURE DEVELOPMENT IN BORON DOPED Ni_3Al

By

Pavan Nagpal

A THESIS

Submitted to

Michigan State University

in partial fulfillment of the requirements

for the degree of

MASTER OF SCIENCE

Department of Metallurgy, Mechanics and Materials Science

1987

ABSTRACT

RECRYSTALLIZATION KINETICS, MICROSTRUCTURE, AND TEXTURE DEVELOPMENT IN BORON DOPED Ni_3Al

By

Pavan Nagpal

Recrystallization texture and microstructural davelopment of Boron doped Ni_3Al rolled to different degrees of deformation were studied. Texture measurements were made on deformed and recrystallized specimens. Also, TEM investigation of deformed and partially recrystallized samples was conducted. The recrystallization temperature was found to be higher (0.55 T_m) than observed in pure metals (0.4 T_m). In one hour, an 80 % cold rolled sample recrystallizes at 625 ^{0}C whereas a 20 % cold rolled sample recrystallizes at 700 ^{0}C. The brass rolling texture suggests that B-doped Ni_3Al may be a low stacking fault material. Very few deformation twins were observed in the electron microscope, but the tendency towards twinning was suggested by frequent occurence of recrystallization twins. The recrystallization texture was not a typical brass recrystallization texture. In fact, it was not a pronounced texture at all. Boron may be responsible for this effect.

ACKNOWLEDGEMENTS

First of all, I wish to express my sincere thanks and appreciaton to my academic advisor, Professor G. Gottstein, for his constant guidance, continous encouragement and valuable suggestions throughout this study. I would also like to thank my friends in the MMM department for their timely help during experimental work.

Finally, the support of U. S. Department of Energy, Office of Basic Science, under grant number DE-FG02-85ER45205 is gratefully acknowledged.

TABLE OF CONTENTS

LIST OF FIGURES

1. INTRODUCTION

The Nickel Aluminide, Ni_3Al, is an intermetallic compound having the $L1_2$ ordered crystal structure [1]. This material has unique properties that makes it attractive for structural applications at high temperatures. Most important, unlike most conventional alloys, the yield strength of Ni_3Al increases with increasing test temperature [2-4]. Despite its attractive properties, fabrication for structural use is precluded by its propensity towards brittle frature in polycrystalline forms [5-7]. The brittleness is associated with intergranular fracture without appreciable plastic deformation within the grains. Small additions of boron considerably improves the ductility of Ni_3Al [8].

Ductilized Ni_3Al is conceived to be a potential material for future high temperature structural applications. For this purpose it will have to be formed into required shapes and will be exposed to high temperature service environments. At some stage of its production process it will be recrystallized to optimize its microstructure or achieve the desired mechanical properties. The current study is to elucidate the kinetics, mechanisms and microstructural development during recrystallization of B-doped Ni_3Al.

It is widely known that recrystallization is a process that causes softening of a deformed metal and facilitates further deformation. The process of recrystallization, seemingly quite simple, is actually complicated by the fact that it is a structure sensitive process. The

texture obtained in the material during deformation is also very important in predicting the mechanisms controlling recrystallisation. The work done here is a part of a larger study of dynamic recrystallization of boron doped Ni_3Al. It confines its scope to static recrystallization kinetics and texture development.

2. LITERATURE SURVEY

2.1 The Material

2.1.1 Mechanical Properties of Ni_3Al

Superlattice alloys (including intermetallic compounds and long range ordered alloys) have been a topic of considerable scientific and engineering interests in recent years. This is due to the fact that many superlattice alloys show unusual mechanical properties, high microstructural stability and high oxidation resistance at high elevated temperatures. A large number of $L1_2$-type compounds (i.e. Cu_3Au crystal structure) show substantial increase in flow strength with increasing temperature [9-10]. This behavior makes these compounds attractive as new heat resisting materials. However, these materials are often subject to intergranular embrittlement. Ni_3Al falls under this class of materials.

Ni_3Al, also, forms an $L1_2$ ordered crystal structure below the peritectic temperature (1395^{o}C). It is the most important strengthening constituent(γ') phase of commercial nickel-base superalloys, and is responsible for their high temperature strength and creep resistance. It has been known for years that single crystals of Ni_3Al are ductile, while its polycrystalline forms are extremely brittle [6,11]. The brittleness of Ni_3Al polycrystals is due to intergranular fracture.

Microalloying, which involves addition of minor concentrations (usually) in the ppm range) of elements to control grain boundary structure or comnposition. Aoki and Izumi [12] first discovered that small boron additions substantially improved the ductility of Ni_3Al at room temperature. By control of boron concentration, alloy stochiometry, and thermomechanical treatment, Liu and Koch [13] reported a tensile elongation exceeding 50% - the highest tensile ductility ever achieved by polycrystalline aluminides. The beneficial effect of boron was also confirmed by Taub, Huang and Chang [14] who tested Ni_3Al foil materials prepared by melt spin technique.

2.1.2 Effect Of Boron On The Strength Of Grain Boundaries

The beneficial effect of boron on the mechanical properties of Ni_3Al seems to be related to its effects on grain boundary properties. Without any addition of boron, Ni_3Al fails by intergranular fracture. With small additions of boron it shows great ductility and fails through a mixture of transgranular and intergranular fracture [15]. According to Schulson and Baker [16] boron, by segregating to the grain boundaries, eases the movement of dislocations within the plane of the boundary . It is based on the view that to propagate slip through a grain boundary it is necessary to push dislocations into the boundary from one side and bring dislocation out into the grain on the other side. In the general case, the orientation of the grains is such that the dislocation that emerges into the grain will have a Burgers vector different from that of dislocation that enters the boundary. A grain boundary dislocation must be left behind whose Burgers vector is vector difference betweeen those

of incoming and outgoing dislocations. If further slip dislocations are to pass through the boundary at the same location, then the strain concentrations represented the boundary dislocations must be removed or spread out, presumably by dislocation motion within the boundary plane. The easier is this motion, the easier will be the propagation of slip. Also, the tendency for cracking will be lower, owing to the reduction in stress concentration, and the ductility will be greater.

2.1.3 The Effect Of Alloy Stochiometry

Alloy stoichiometry has a strong effect on the ductility and fracture behavior of boron-doped Ni_3Al [15]. Boron is most effective in improving the ductility and supressing intergranular fracture in Ni_3Al containing 24 at.% Al [Figs. 1. and 2.].

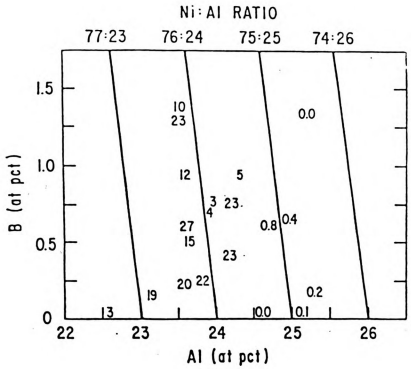

Fig. 1. Plastic strain to fracture (%) of rapidly solidified Ni_3Al - B as a functionb of Al and B concentration.

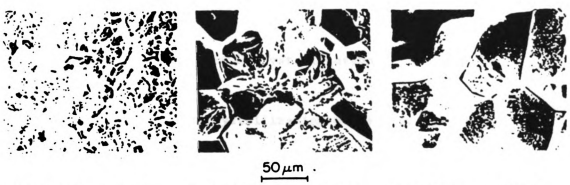

Fig. 2. Effect of stoichiometry on fracture mode of B - doped Ni_3Al at room temperature.

2.2 Recrystallization

2.2.1 General Definition

Primary recrystallization is defined as the nucleation and growth of strain free grains from a deformed microstructure (It is actually rebuilding of the crystalline structure by generation and motion of high angle grain boundaries from the deformed state with concomittant elimination of the dislocation structure).

Primary recrystallization diminishes the number of structure defects caused by prior deformation, and restores the properties the metal had before deformation.

The main driving force for primary recrystallization is the elastic energy stored in the strain field of the dislocation which comprise the deformed structure.

2.2.2 Nucleation Of Primary Recrystallization.

The characteristics of recrystallization nucleation are :

a) Nucleation of the new state is irreversible and the initial state cannot be restored.

b) The size of the viable nuclei is microscopically small and its configuration preformed in the deformed structure.

c) Nucleations occur in regions which deviate from the average structure.

The following nucleating mechanisms have been proposed:

[1]) Nucleation by strain induced grain boundary motion (SIBM).

A preexisting grain boundary in a polycrystal may bulge when an imbalance of driving force is introduced. Since bulging increases the grain boundary area the bulge must exceed a critical radius in order to gain energy on further growth. SIBM has been observed to occur only at low degrees of deformation as shown below Fig. 4.

[2]) Nucleation at deformation inhomogeneties [Figs. 3. and 5.].

During deformation band shaped inhomogeneties are formed (kink bands, deformation bands, shear bands etc.). The transition from band to matrix is generally accomodated by elongated subgrains with small but additive orientation differences. The growth of one subgrain in the transition region leads to a high angle grain boundary.

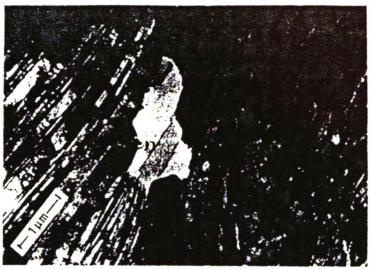

Fig. 3. TEM micrograph of a nucleus at the boundary of a shear band in rolled Cu.

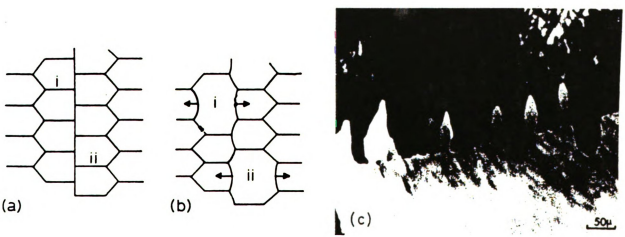

Fig. 4. Recovery induced SIBM by local subgrain coalesence at a grain boundary. (a) before, (b) after coalesence. (c) SIBM in 40% compressed Al.

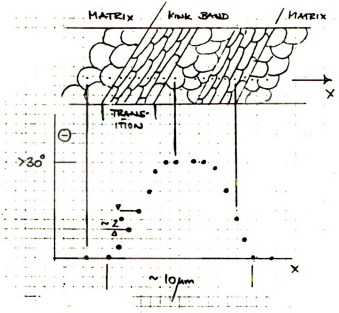

Fig. 5. Schematic diagram showing transition from band to matrix with small but additive orientation differences.

[3]) Production of grains with orientation not preexisting in the deformed structure.

One example is the so called Rowland transformation by which two twin related crystals collapse to form a common orientation. This mechanism was suggested for the formation of the cube texture. The feasibility of this mechanism has been doubted, however, and there is little evidence to support this model.

High angle grain boundary can also be created by twin formation. TEM observations have established that annealing twins are formed at a very early state of recrystallization. They are emitted from subboundaries and can produce a high angle boundary. Within the twins second, third or fourth order twins can be formed [19] providing a highly mobile grain boundary [Fig. 6.].

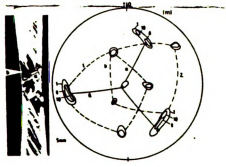

Fig. 6. Micrograph and [111] pole figure of a Cu single crystal dynamically recrystallized at 560 °C showing a twin family. Grain (a) (dashed orientation) is a primary twin to the deformation structure, and grain (b) (dashed-dotted orientation) a twin of (a).

2.2.3 Recrystallizaton Kinetics

The recrystallization temperature is generally understood as the temperature where recrystallization has been completed in one hour.

The recrystallization volume fraction can be measuured by structure sensitive physical properties like electrical resistivity, specific heat or flow stress (hardness). The relative change of a property is generally believed to be proportional to the recrystallized volume fraction.

After annealing for time t, the recrystallized volume fraction X(t) is given by

$$X(t) = \frac{h(t) - h_0}{h_E - h_0}$$

where

$h(t)$ = The measured quantity after time t

h_0 = h (t=0)

h_E = h (t=∞)

Schematic curves of recrystallization are shown below [Fig. 7.].

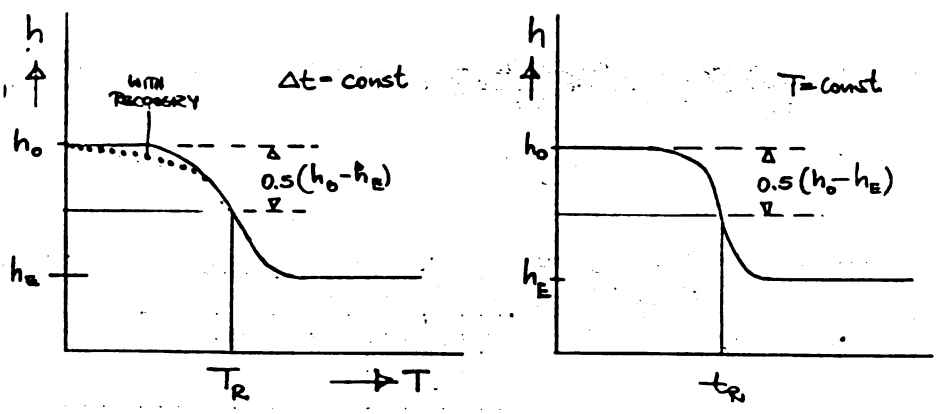

Fig. 7. Schematic curves of recrystallization in hardness.

2.2.4 Recrystallization In Ordered Alloys

Recrystallization kinetics have been reported for a very few ordered alloys [20], a warm worked intermetallic compound in polycrystalline form [21] and a cold worked one in a single crystal form [22].

Takasugi and Izumi [23] observed that recrystallization and grain growth occurs in polycrystalline Co_3Ti ($L1_2$ structure). The critical temperatures for recrystallization and grain growth were quite high, as shown in the figs. 8 & 9. Solute atoms drastically reduce the mobility through a sort of solute atmosphere near the grain boundary [24]. Excess Co atoms in the off-stoichiometric Co_3Ti can be regarded as solute atoms. Therefore lower rate of recrystalliztion is assumed to be due to interaction of grain boundary with Co atoms.

Schulson and Haff observed that warm worked NiAl recrystallizes and undergoes subsequent grain growth in a manner typical of metals and alloys [21]. The decrease in hardness coressponds to the increase in recrystallized area as seen in Fig. 10.

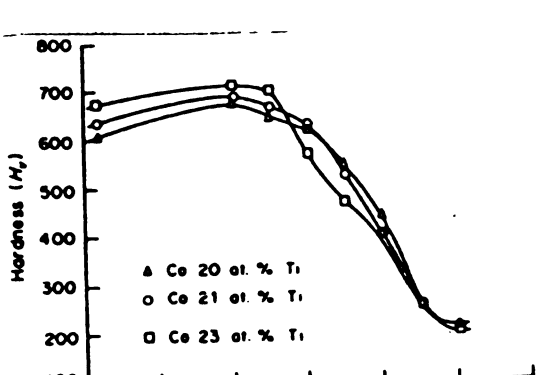

Fig. 8. Isochronal annealing (for 2h) curves in the hardness for for specimens of Co_3Ti cold-rolled to ϵ = 50%.

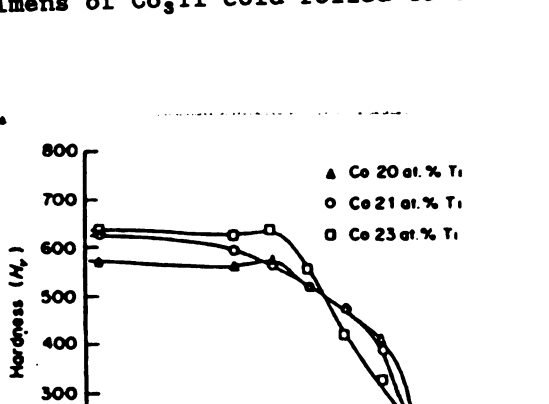

Fig. 9. Isochronal annealing (for 2h) curves in the hardness for the specimens of Co_3Ti colled rolled to ϵ = 80%.

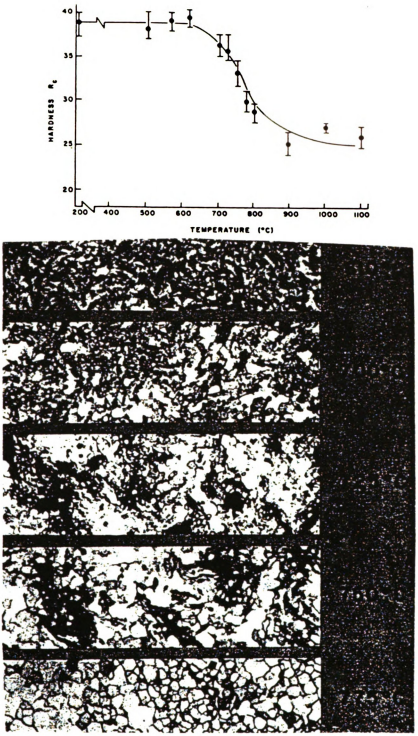

Fig. 10. Optical micrographs illustrating the microstructural changes accompanying the isochronal anneals of NiAl.

3. EXPERIMENTAL PROCEDURE

3.1 Testing Material

A casting prepared by arc-melting several times in an argon atmosphere to promote homogenity and then drop-cast in a copper mold, of the following composition was used. The composition of the final casting was as follows:

Ni	76 at. %
Al	24 at. %
B	.24 at. %

3.2 Specimen Preparation

3.2.1 Cold Rolling And Annealing

Experiment 1 : Isochronal Annealing.

A Specimen was cut from a B-doped Ni_3Al casting by abrasive wheel cutter. This was then rolled at room temperature in steps of .3 - .4 mm initially. Cracks were observed after 23% reduction in thickness. Further reduction was given in minimum steps of .1 - .2 mm to avoid cracking. Maximum reduction of 72% was possible since extensive cracking was observed.

Samples of the rolled sheet were isochronally annealed in air for 15 minutes between $700^{0}C$ and $1000^{0}C$.

Experiment 2 : Isothermal Annealing.

Another specimen was similarly rolled at room temperature to 80 % reduction, upon which the specimen had cracked extensively. A sample was cut after 18 %, 40 %, 60 % reductions.

These samples were then isothermally annealed in air at 700 ^{0}C upto 60 minutes.

Experiment 3 : This sample was homogenized at 1050 ^{0} C for an hour. Then it was rolled to 20, 40, 60 and 80 percentage reductions. Further, samples were isothermally annealed at 600, 625, 650 and 675 degree celsius.

3.2.2 Texture Measurement

Samples rolled to 80% and 90% reduction were used to determine the deformation texture. The surface of the samples were etched to eliminate surface effects. {111} and {200} pole figures were measured using an x-ray goniometer.

3.2.3 Optical Microscopy

Experiment 1 : The samples were etched in the following solution :

Nitric Acid	20 ml
Phosphoric Acid	20 ml
Distilled Water	20 ml
Acetic Acid	10 ml
Hydroflouric Acid	10 ml
Hydrochloric Acid	10 ml

The sample was immersed in a solution heated to 45°C for 30s. The microstructures were seen along rolling plane normal.

Experiment 2 & 3 : These samples were etched in Marble 's reagent (composition shown below) at room temperature for 5s. The microstructures were seen along the transverse direction.

Marble's reagent :

$CuSo_4$: 5g

HCl : 20 ml

H_2O : 20 ml

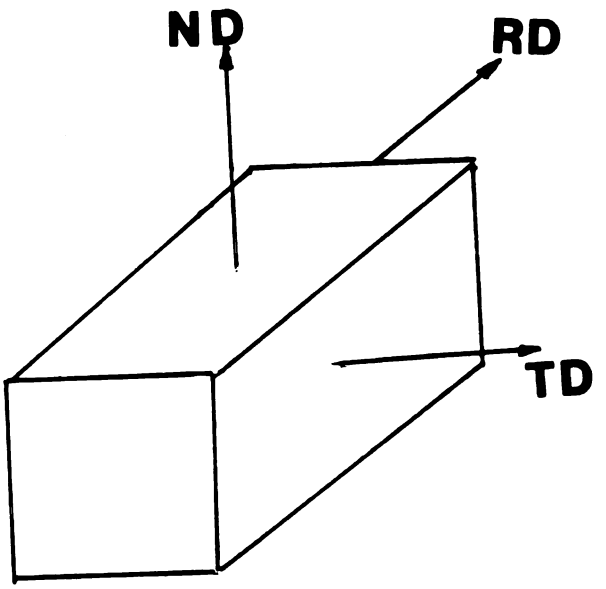

Fig. 11. Schematic diagram showing rolling configuration.

3.2.4 Electron Microscopy

Rolled and partially recrystallized samples were reduced in thickness to 500μm by grinding and then mechanical polished to 150μm. Disks of 3mm in

diameter were cut by electron discharge machine. These samples were then electropolished in the following solution:

Perchloric Acid	150 ml
Distilled Water	875 ml
Butoxy Ethanol	150 ml
Ethanol	946 ml

Voltage: 27 V Temp.: 10-12 ^{o}C

Current (important): 0.23-0.25 amps.

3.3 Hardness Testing

(1) For the Isochronal test, Rockwell hardness was measured. The Rockwell values were converted into Brinell hardness number (BHN) by using the following relations:

B35-B100:

$$BHN = \frac{7300}{130-R_B}$$

C20-C40:

$$BHN = \frac{142000}{(100-R_C)^2}$$

>C40:

$$BHN = \frac{25000}{100-R_C}$$

(2) Microhardness tests were employed for the remaining experiments. A diamond pyramid hardness tester was used to measure the change on

hardness on annealing. The diamond pyramid hardness number (DPH) was determined from the following equation [24]:

$$DPH = \frac{2P\sin(\theta/2)}{L^2} = \frac{1.854P}{L^2}$$

where

P = applied load, Kg

L = average length of diagonal, mm

θ = angle between opposite faces of diamond = 136^{o}

Applied load was 0.5 Kg

At least five identations were made. Care was taken to discard indentations near the cracks.

4. EXPERIMENTAL RESULTS

4.1 Recrystallization Behavior

Fig. 12 shows the hardness of a 72 % cold rolled specimen isochronally annealed for 15 minutes at temperatures upto 1000°C. No change in hardness occurs upto 650°C. The rise in hardness between 550°C and 650°C is misleading. The curve is drawn by a computer using a spline which results in the peculiar shape. Between 650°C and 700° C, there is a drastic drop in hardness and then it continues to drop steadily till 1000°C.

Fig. 13 shows the change in hardness on isothermal annealing at 700°C for different degrees of deformation. The curve for 80% cold rolling shows the steepest drop in 10 minutes. The hardness decreases steadily till 50 minutes. For 60, 40, and 20 % cold rolling curves, there is a considerable change within 20 minutes of annealing. Then the hardness remains almost constant for an hour. A slight increase in hardness for 20 % cold rolling curve may be due to the area where the indentation was made.

Isothermal annealing curves at 625 deg C for 40 and 60 % cold rolled specimen are shown in fig. 14. The 60 % cold rolling curve shows no change in hardness until 15 minutes and then continues to drop till 45 mins. The 40 % cold rolling curve shows a slight drop in 15 mins. and it remains steady till 45 mins.

Fig. 15 shows isothermal annealing curves for 80 % cold rolled specimen at different temperatures. At 625 ^{0}C, there is no change in hardness even after 25 minutes of annealing . A considerable change in hardness is observed after 55 mins. of annealing. At 650^{0}C, no drop in hardness is seen till 10 minutes. Between 10 and 35 mins., the hardness decreases considerably. The 675^{0}C curve shows a steady drop in hardness till 35 mins. of annealing.

4.2 Microstructural Development

4.2.1 Isochronal Test:

For the isochronal test on a 72 % cold rolled sample, very fine recrystallized grains of less than 1μm grain size were observed after annealing for 15 minutes at 700^{0}C [fig. 12]. The grain size increases to about 15μm after annealing for 15 min. at 950^{0}C [fig. 16 d].

4.2.2 Isothermal Tests:

A. 80 % cold rolling

Extremely fine grains are seen after isothermal annealing for 20 min. at 700^{0}C. The microstructure looks almost similar on further annealing for 40 minutes [fig. 17 b]. On lowering the temperature, 675^{0}C, higher amount of unrecrystallized area is seen after 15 mins. of annealing [fig.]. At 650^{0}C, few unrecrystallized grains are seen after annealing for 40 mins. [fig. 17 f]. Very few recrystallized grains are seen after

of annealing at 625 ^{0}C. The specimen is almost completely recrystallized after after 55 mins.

B. 60 % cold Rolling

The deformed structure of 60 % cold rolled sample is seen in fig. 18 a. Grains are oriented towards the rolling direction. Completly recrystallized grains are observed after annealing for 45 mins. at 700^{0}C [fig. 18 b] whereas at 625^{0}C are still seen after annealing for 45 mins. [fig. 18 c].

C. 40 % cold rolling

Fig. 19 a shows the 40 % cold rolled structure. New grains are seen at the grain boundaries after 20 mins. of annealing at 700^{0}C [fig. 19 c]. These grains grow on further annealing till 50 min. [fig. 19 f]. After annealing for 45 mins. at 625^{0}C, only few grains are seen at the grain boundaries [fig. 19 b].

D. 20 % cold Rolling

Fig. 20 a shows the slightly elongated grains of a 20 % cold rolled structure. There is no change in microstructure after 20 min. of annealing at 700^{0}C. [fig. 20 b]. Further annealing of 10 min. shows some grain boundary migration [fig. 20 c]. New grains are seen near the surface of the sample[fig. 20 d]. This may be due to the surface being more deformed that the bulk owing to friction on the surface and small thickness reductions. After 50 min. at 700^{0}C , new grains are seen in the interior of some grains [fig. 20 e].

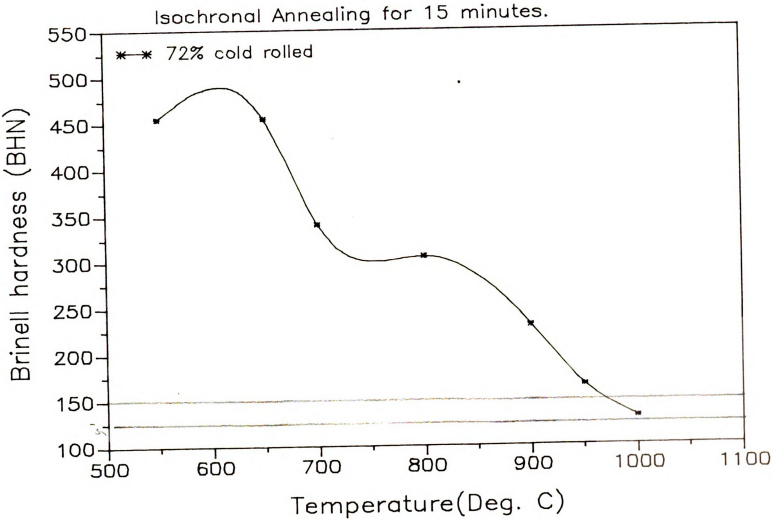

Fig. 12. Isochronal annealing (for 15 minutes) curve in the hardness for the 72% cold rolled specimens.

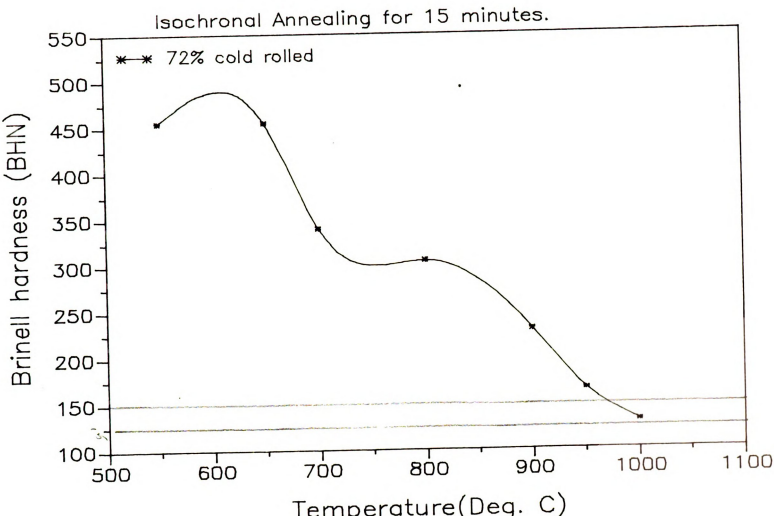

Fig. 12. Isochronal annealing (for 15 minutes) curve in the hardness for the 72% cold rolled specimens.

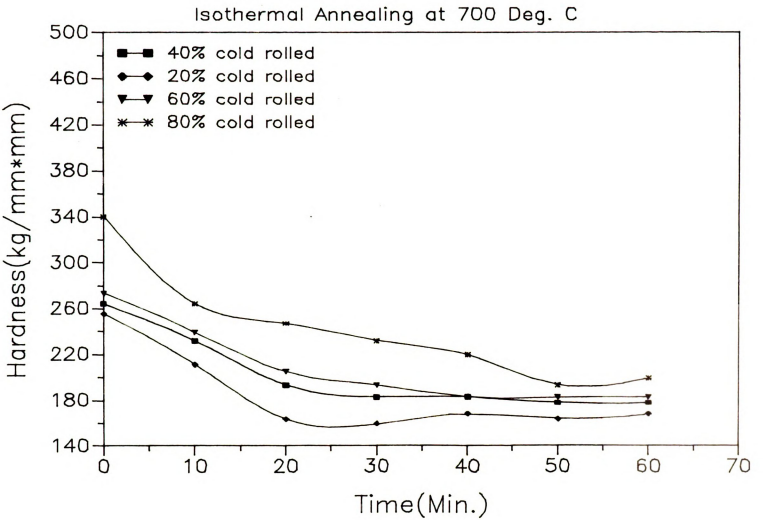

Fig. 13. Isothermal annealing curves at 700°C with different degrees of deformation.

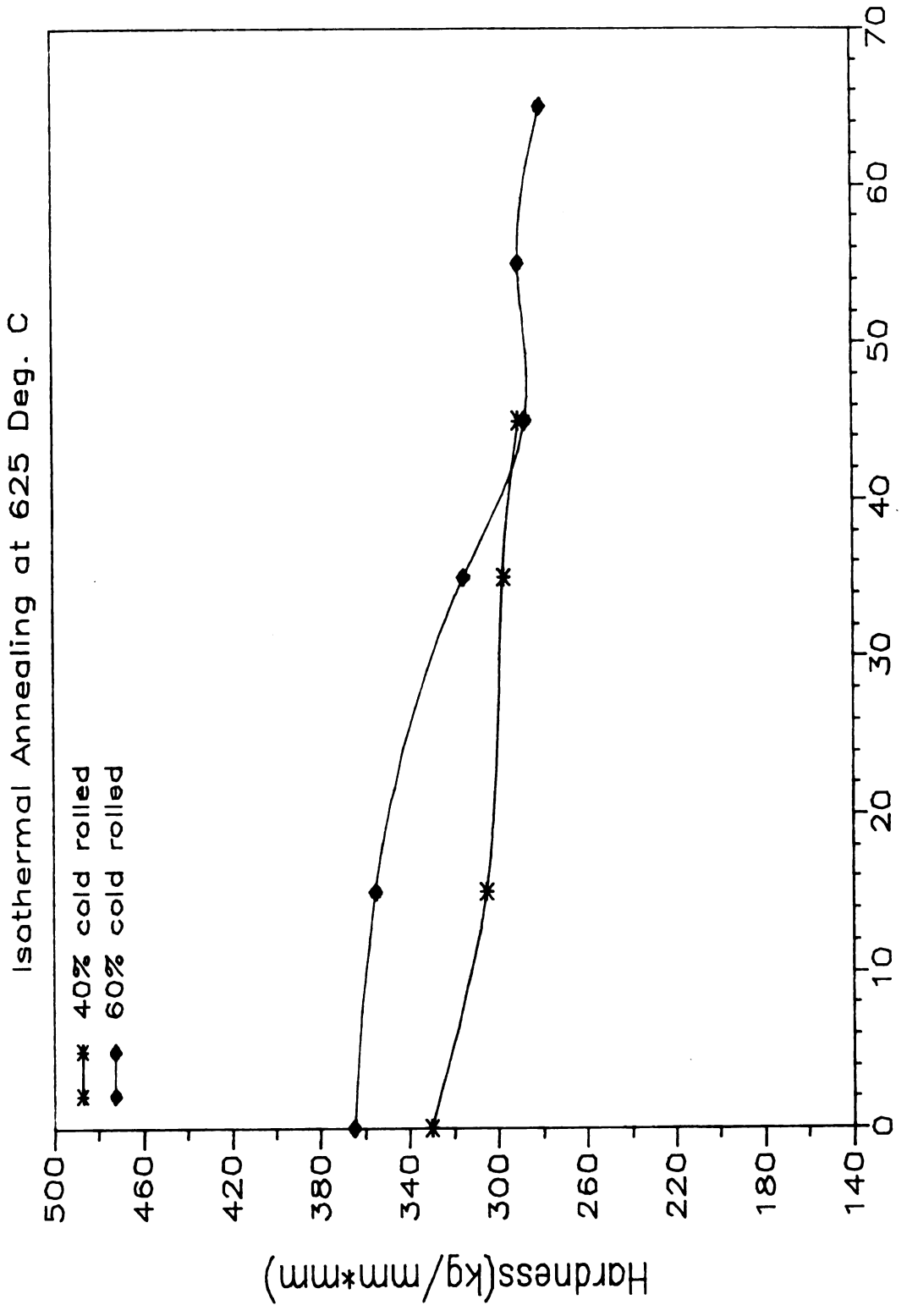

Fig. 14. Isothermal annealing curves at 625°C with different degrees of deformation.

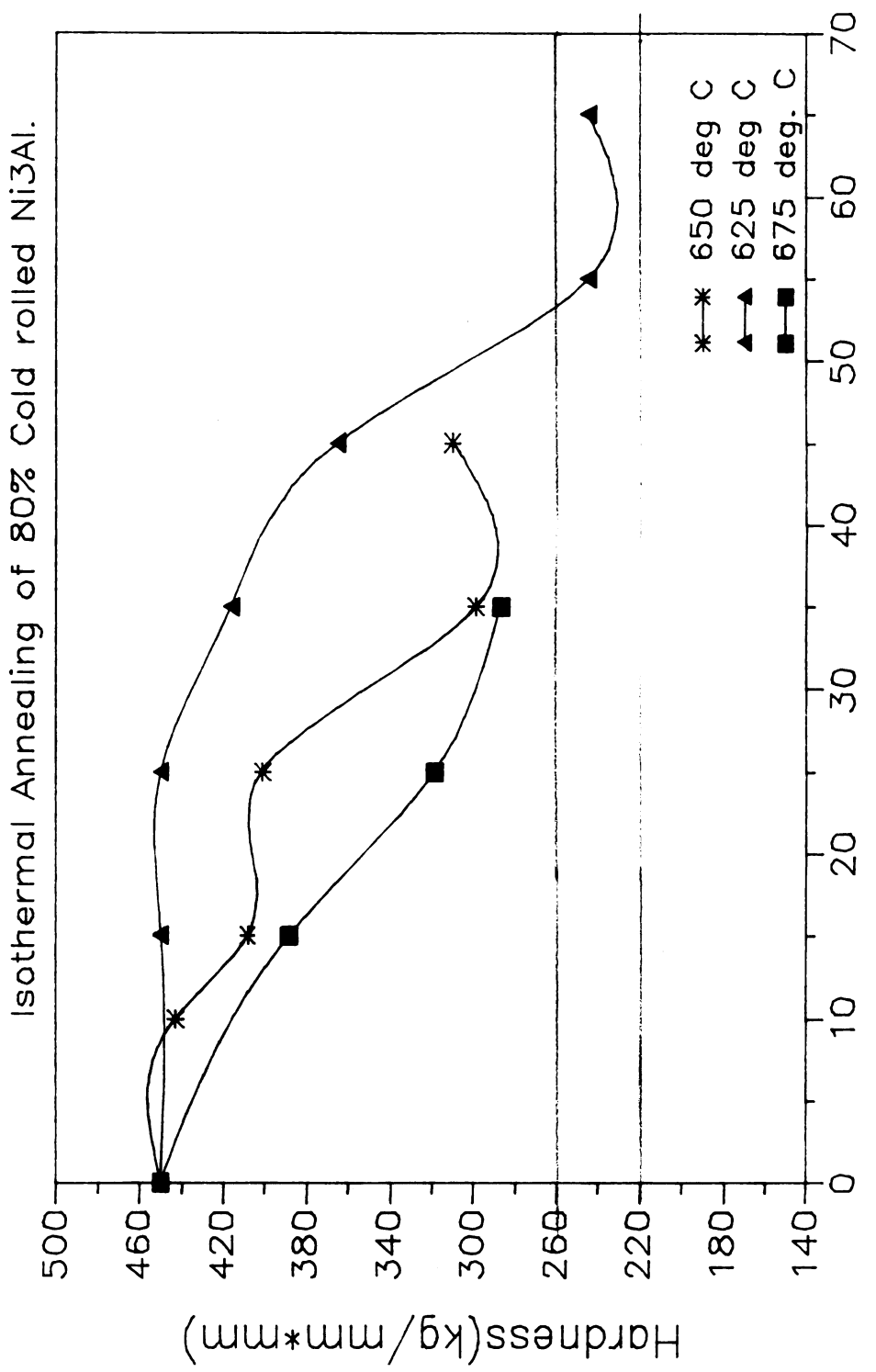

Fig. 15. Isothermal annealing of 80% colled rolled specimens at 625, 650 and 675 deg. C.

Fig. 16 Optical micrographs illustrating microstructural changes accompanying isochronal annealing of 72% cold rolled specimens:

a) for 15 min. at 700°C.

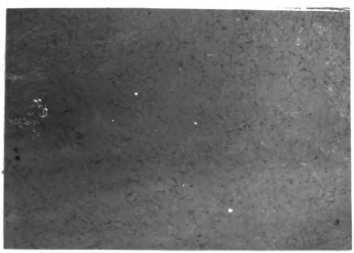

b) for 15 min. at 800°C.

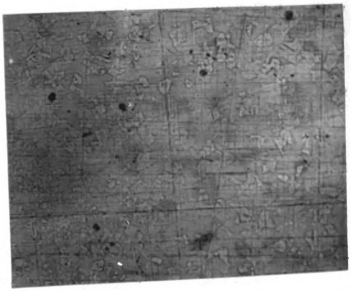

c) for 15 min. at 900°C.

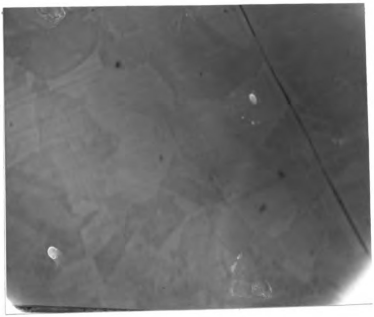

d) for 15 min. at 950°C.

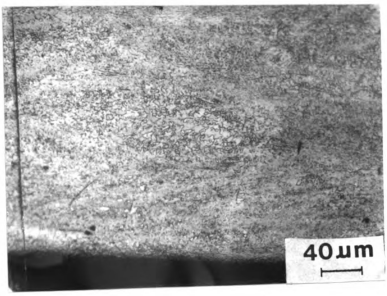

Fig. 17. Optical micrographs illustrating microstructural changes accompanying isothermal annealing of 80% cold rolled specimens:

a) after 20 min. at 700°C.

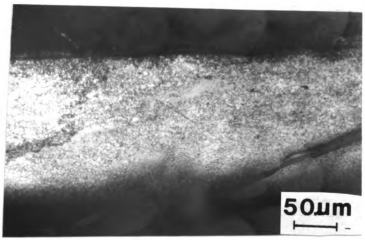

b) after 40 min. at 700°C.

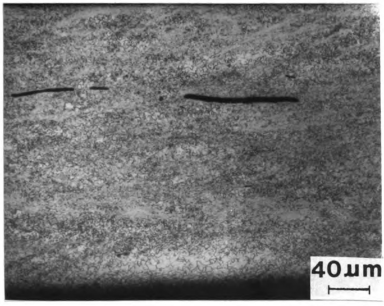

c) after 50 min. at 700°C.

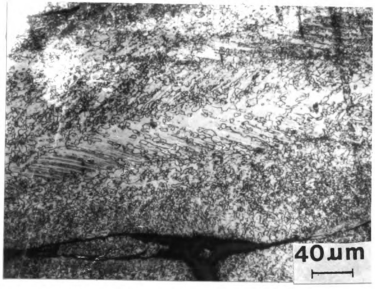

d) after 15 min. at 675°C.

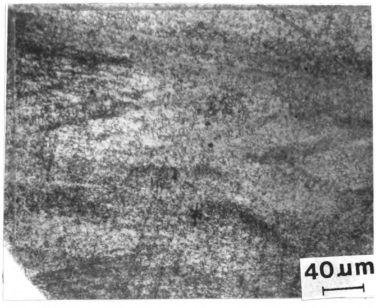

e) after 25 min. at 675°C.

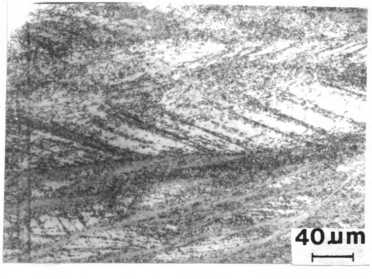

f) after 40 min. at 650°C.

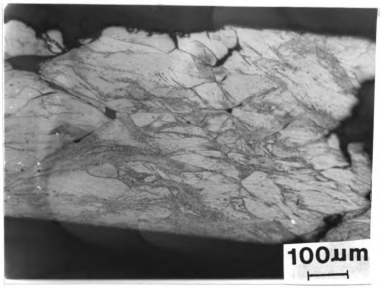

g) after 10 min. at 625°C.

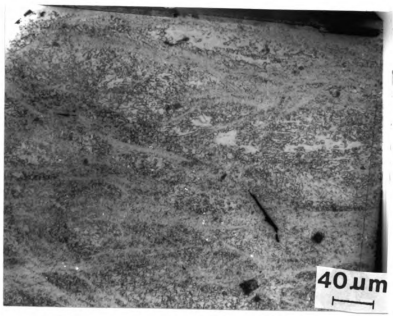

h) after 55 min. at 625°C.

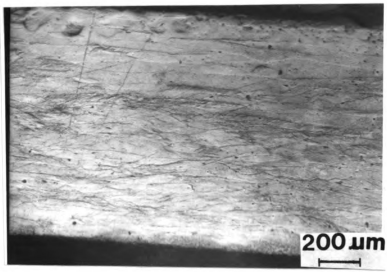

Fig. 18. Optical micrographs illustrating microstructural changes accompanying isothermal annealing of 60% cold rolled specimens.
a) as rolled

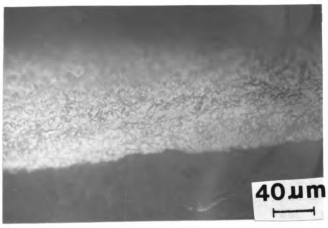

b) after 45 min. at 700 °C.

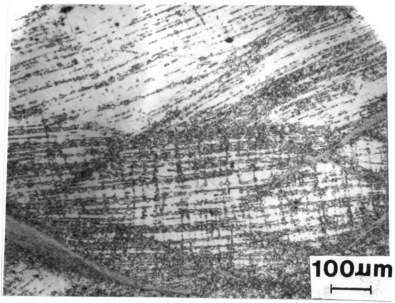

c) after 45 min. at 625 °C.

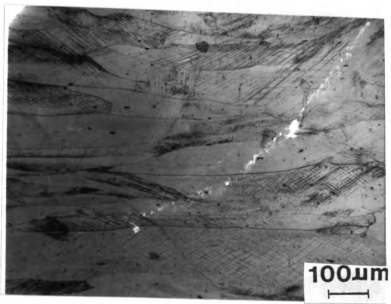

Fig. 19. Optical micrographs illustrating microstructural changes accompanying isothermal annealing of 40% cold rolled specimens:

a) as rolled.

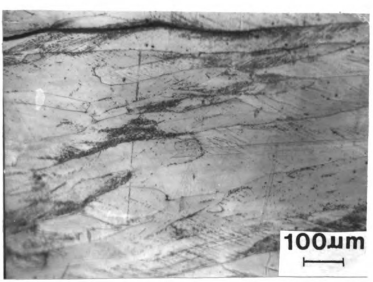

b) after 45 min. at 625 ^{o}C.

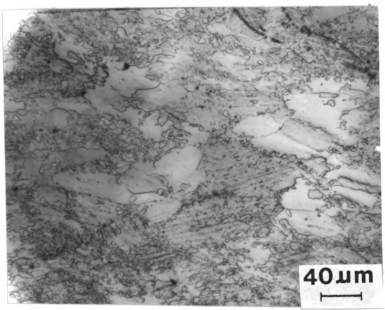

c) after 20 min. at 700°C.

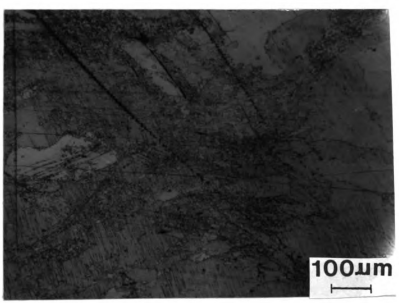

d) after 30 min. at 700°C.

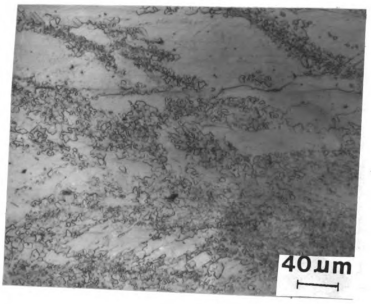

e) after 40 min. at 700°C.

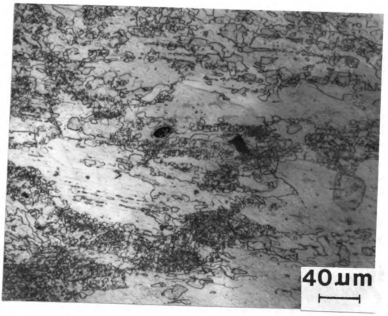

f) after 50 min. at 700°C.

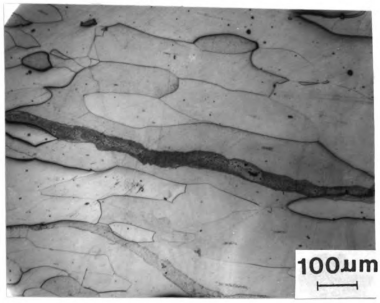

Fig. 20. Optical micrographs illustrating microstructural changes accompanying isothermal annealing of 20% cold rolled specimens:

a) as rolled

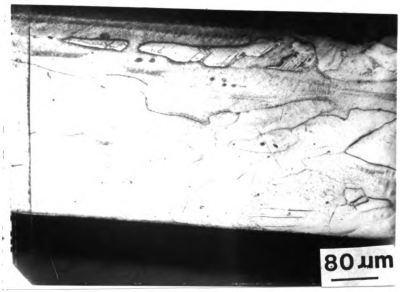

b) after 20 min. at 700°C.

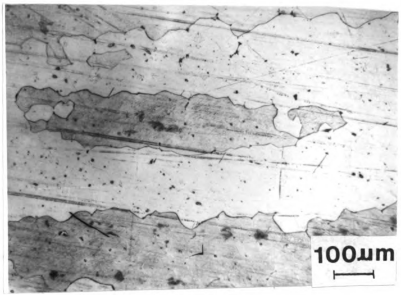

c) after 30 min. at 700°C.

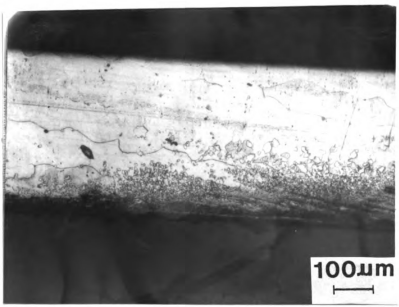

d) after 40 min. at 700°C.

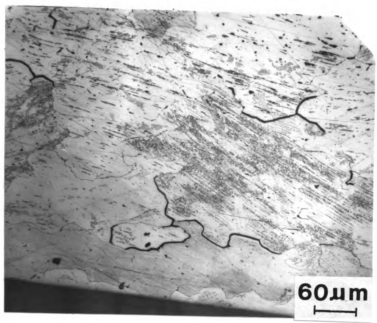

e) after 50 min. at 700°C.

4.3 Texture Measurement

Fig. 21 shows (111) and (200) pole figures of 90 % cold rolled specimen. Both the pole figures show a stronger goss component and a weaker brass component. Fig. 22 shows the (111) and (200) pole figures of fully recrystallized specimen. There is no pronounced texture at all.

4.4 Transmission Electron Microscopy

Figs. 23 show a partially recrystallized structure of a specimen rolled to 75 % and annealed at 625^{0}C for 10 mins. Large grains are seen surrounded by the deformed matrix.

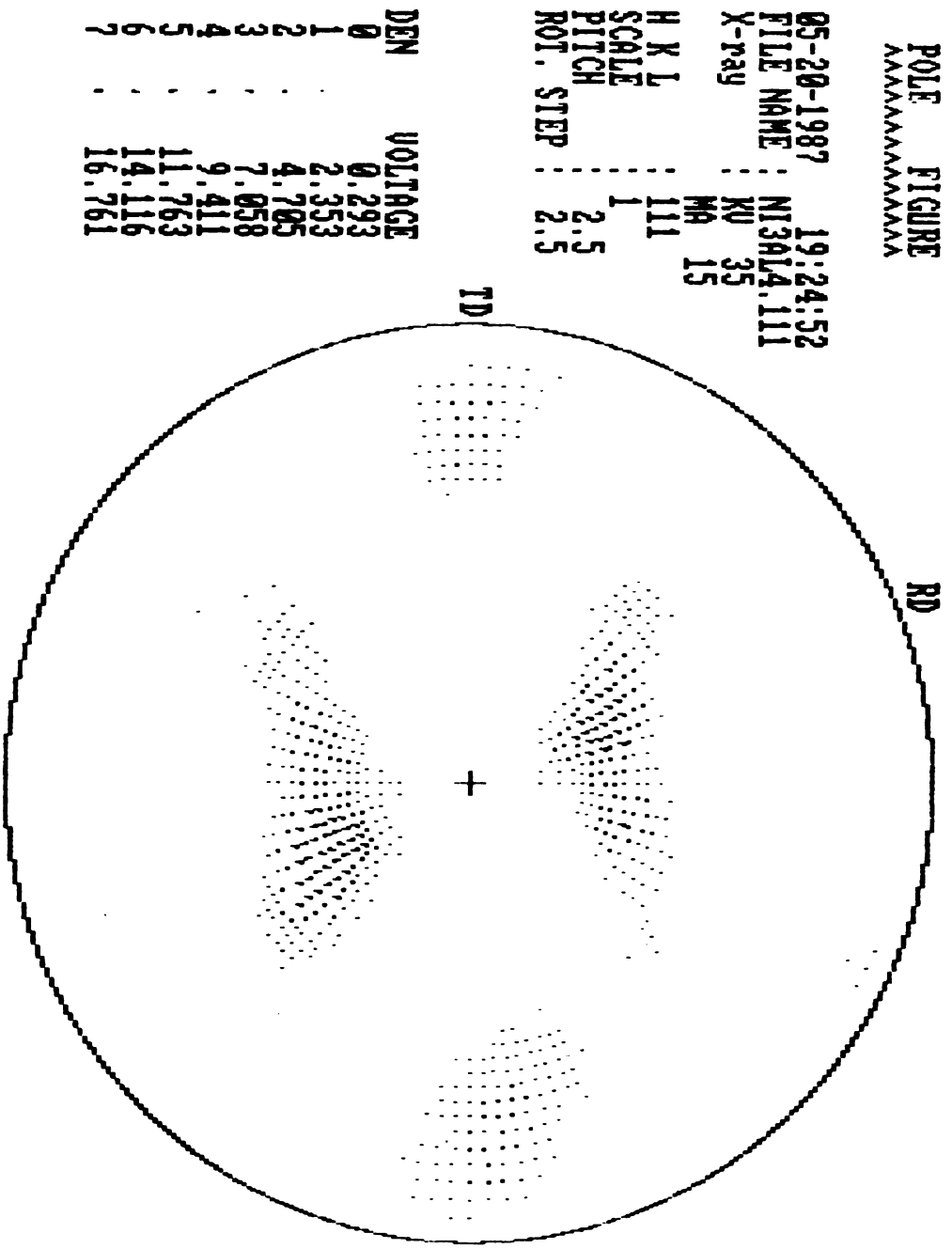

Fig. 21. Pole figure of 90 % cold rolled specimen.
a) (111).

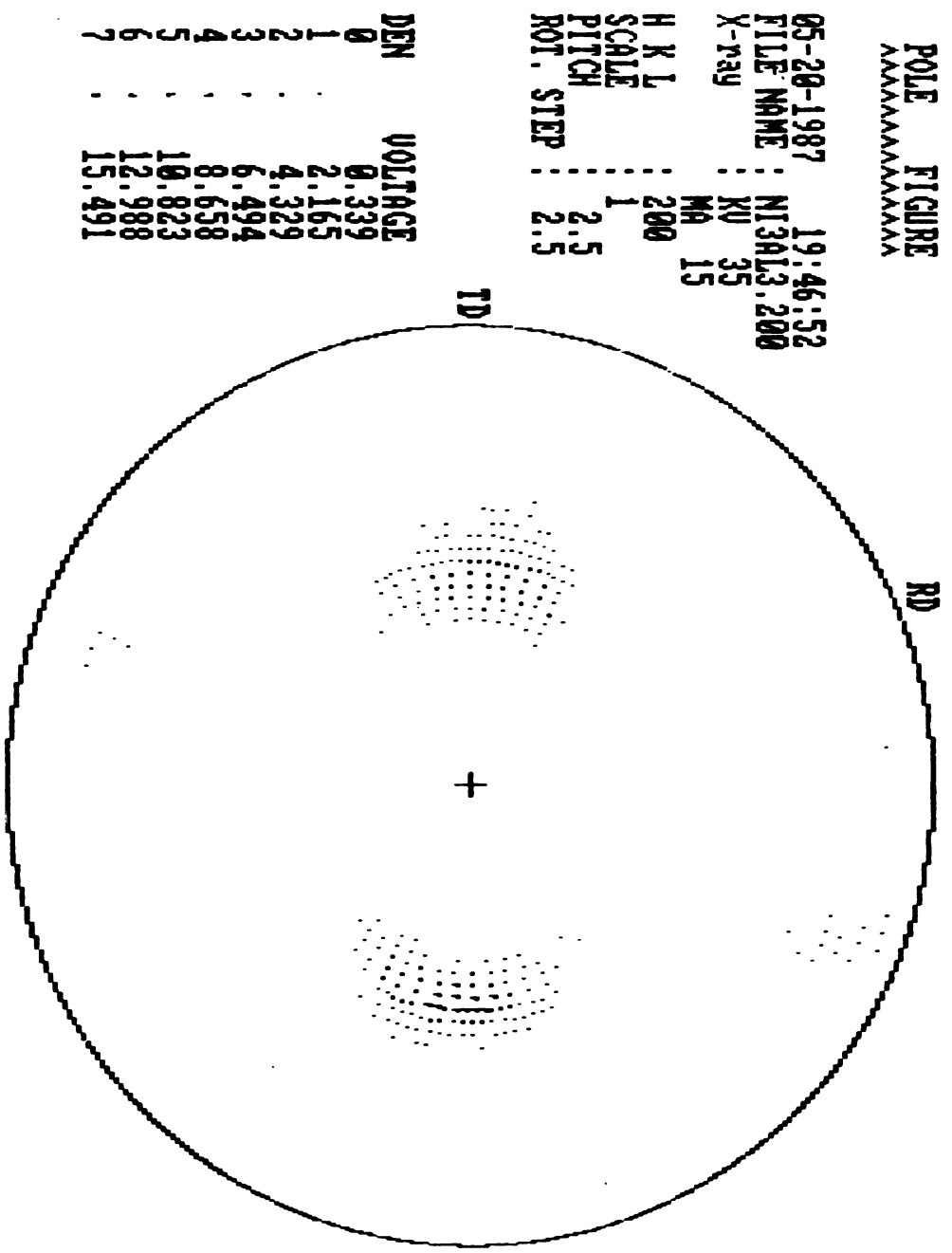
POLE FIGURE
05-20-1987 19:46:52
FILE NAME : NI3AL3.200
X-ray : KU MA
H K L : 2 0 0
SCALE : 1
PITCH : 2.5
ROT. STEP : 2.5
DEN VOLTAGE
0 0.339
1 2.165
2 4.329
3 6.494
4 8.658
5 10.823
6 12.988
7 15.491
TD
RD

b) (200).

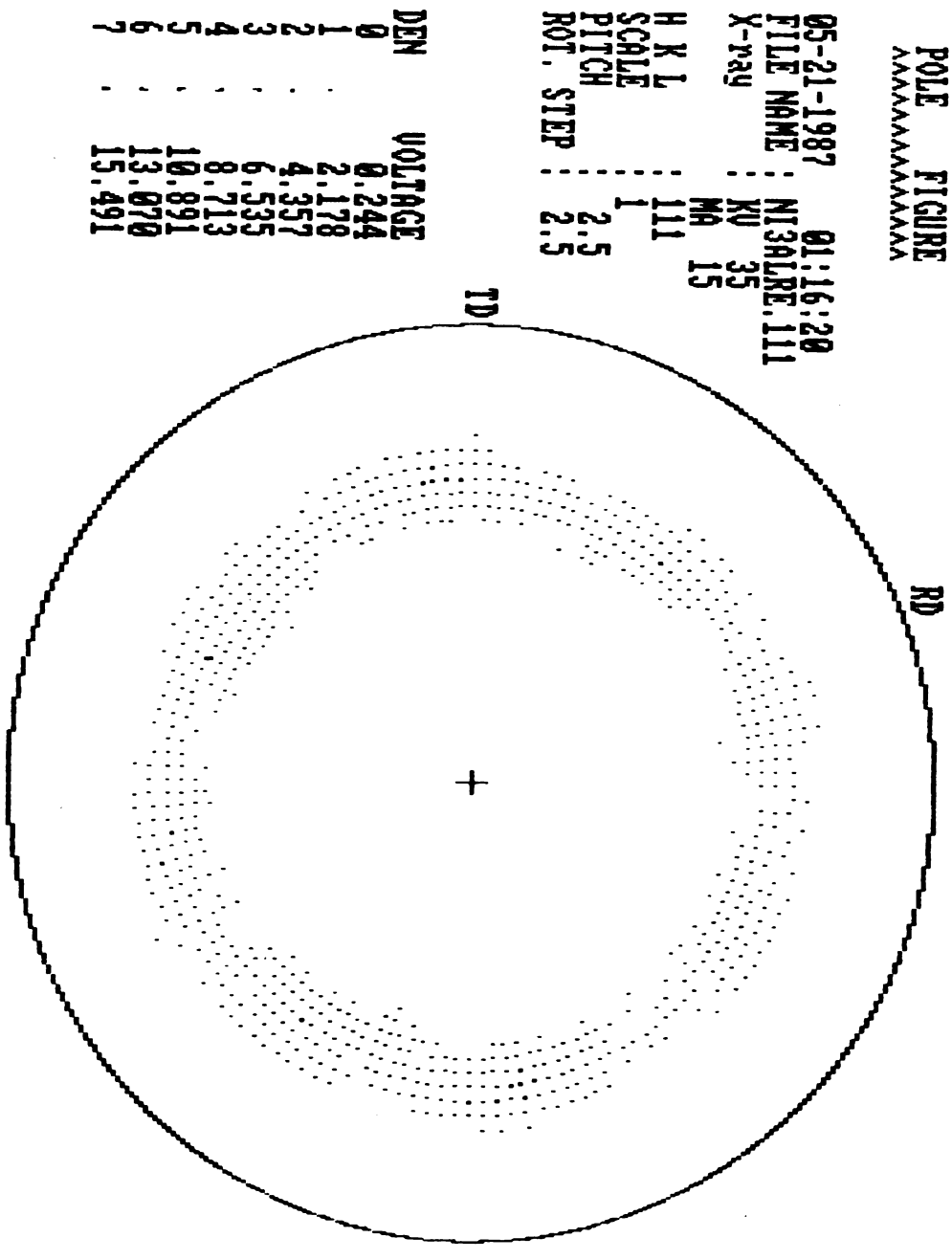

Fig. 22. Pole figure of fully recrystallized specimen.
a) (111).

POLE FIGURE
AAAAAAAAAAAAA
05-21-1987 01:23:19
FILE NAME : NI3AlRE.200
X-Ray : KU 35
MA 15
H K L : 200
SCALE : 1
PITCH : 2.5
ROT. STEP : 2.5
RD
TD
DEN VOLTAGE
0 0.194
1 0.461
2 0.921
3 1.382
4 1.842
5 2.303
6 2.764
7 3.418

b) (200).

Fig. 23. TEM micrograph showing a partially recrystallized structure.

5. DISCUSSION

5.1 Recrystalliztion Behaviour

5.1.1 Isochronal Test

Complete recrystallization is occurs within 15 mins. of annealing at 700^{0}C. The continual drop in hardness may be due to a grain size strengthening affect. Firstly, the Hall-Petch coefficient, K, is very high [25]. Secondly, there is a substantial grain growth from <1μm to 15μm.

5.1.2 Isothermal Tests

The recrystallization behavior, as revealed by isothermal annealing curves and microstructures, is affected by the degree of deformation and the temperature of annealing. For a constant temperature, increasing the amount of cold work enhances the rate of recrystallization. Since nucleation occurs at deformation inhomogenities which increase with increasing cold work, therefore nucleation rate increases and hence the rate of recrystallization. For a constant amount of cold work, increasing the temperature also increases the rate of recrystallization. Higher temperatures have two fold effects. One, by enhancing recovery processes nucleation rate is increased. Two, by increasing grain boundary mobility, the growth rate increases.

Regarding nucleation of new strain free grains, the mechanism varies depending on the degree of deformation.

a. High degree of deformation (80 % cold rolling)
At large degrees of deformation, shear bands form within the grains. These bands have dislocatin density and large difference in orientation with the matrix. Therefore they act as nucleation sites as shown in figs. 17 f and 18.

b. Intermediate degree of deformation (40 %)
At moderate amounts of deformation, a higher dislocation density exists near the grain boundary than the grain interior. Thus nucleation mainly occurs at the grain buoundaries [fig. 19 c & d].

c. Low degree of deformation (20 %)
Dislocation density is much lower at small amounts of deformation. But, the difference in dislocation densities between adjacent grains induces so called strain induced boundary migration (SIBM) [figs. 20 c & d]. Some grains whose boundaries moved during SIBM also showed new recrystallized grains in their interior [fig. 20 e] which indicates that locally the dislocation density is high enough and the arrangement liable enough to nucleation of recrystallized grains.

5.2 Texture Measurement

The rolling texture is a brass type texture, which is usually found in low stacking fault energy materials at low temperatures. It is typical for concentrated alloy. The result indicates that Ni_3Al has to be

classified as a low stacking fault energy material. This is surprising, since a stacking fault concurrently creates an antiphase boundry so that the stacking fault energy includes an antiphase boundry energy.

The electron microscopy of deformed and partially recrystallized sample did not reveal a strong tendency toward twinning. Actually deformation twins were rarely seen in our samples, but the propensity toward twinning is indicated by the frequent occurrence of recrystalliztion twins, even in the early stage of recrystallization.

The recrystallization texture is not a brass recrystallization texture. It is not a pronounced texture at all. Boron, because of impurity drag , may reduce the grain boundary migration rate. It is known that boron strongly segregates to grain boundaries and therefore should exert a substantial grain boundary drag. Also the presence of boron in the boundary can alter the structure of the boundary and thus, affect the grain boundary mobility.

6. CONCLUSIONS

1. The recrystallization behavior is fundamentally similar to pure metals and alloys. However, the recrystallization temperature was higher (0.55 T_m) than pure metals (0.4 T_m).

2. An 80 % cold rolled specimen recrystallizes at 625 ^{o}C in one hour.

3. A 20 % cold rolled specimen recrystallizes at 700 ^{o}C in one hour.

4. Although the brass rolling texture may suggest a low stacking fault energy material, very few deformation twins were observed in the electron microscope. However, tendency toward twinning was suggested by the frequent occurence of recrystallization twins, even in the early stage of recrystallization.

5. The recrystallization texture was not a typical brass recrystallization texture. It was not a pronounced texture at all. Boron, by impurity drag, may be responsible for reducing the grain boundary migration rate.

7. REFERENCES

1) M. Hansen, constitution of binary alloys, pp. 119, McGraw Hill Book company, New York (1958).

2) P. H. Thorton, R. G. Davis and T. L. Johnson, Metall. Trans. 1, 207 (1970).

3) P. A. Flinn, Trans. TMS. AMIE 218, 145 (1960).

4) R. G. Davis and N. S. Stoloff, Trans. TMS. AMIE 233, 714 (1965)

5) R. Moskovic, J. Material Sci. 13, 1901 (1978)

6) K. Aoki and O. Izumi, Trans JIM 19, 203 (1978).

7) A. V. Seybolt and J. H. Westbrook , Acta. Metall. 12, 449 (1964).

8) K. Aoki and O. Izumi, Nippon Kizaku Gakkaishi, 43, 1190 (1979).

9) E . M. Schulson and J. A. Roy , Acta Metall. 26, 29 (1978)

10) S. Takeuchi and E. Kuramuto, Acta. Metall. 21, 415 (1973)

11) K. Aoki and O. Izumi, Nippon Kinzoku Gakkashi 41, 170 (1977)

12) K. Aoki and O. Izumi, Nippon Kinzoku Gakkashi, 43, 1190 (1979

13) C. T. Liu and C. L. White, C. C. Koch and E. H. Lee, Proc. symp. high temperature materials chemistry II, ed. Mumir, et al. , the electrochemical soc. , Inc. (1983)

14) I. Taub, S. C. Huang and K. M. Chang, Metall. Trans. A. 15A, 399 (1984)

15) C. T. Liu, C. L. White and J. A. Horton, Acta. Metall. 33, 213 (1985)

16) E. M. Schulson, T. P. Weihs, I. Baker, H. J. Frost and J. A. Horton Acta. Metall. 34, 1395 (1986)

17) G. Gottstein, Preferred orientation in deformed metals and rocks: An Introduction to Modern Texture analysis.

18) G. Gottstein D. Zabardjadi and H. Mecking, Metal Sci. 13, 223 (1979).

19) M. Gagne and E. M. Schulson, Metall. Trans. 7A, 1775 (1976).

20) G. R. Haff and E. M. Schulson, Metall. Trans. 23A, 1563 (1982).

21) K. Aoki and O. Izumi, Trans. Japan Inst. Metals 19, 203 (1978).

22) T. Takasugi and O. Izumi, Acta. metall. 33, 49 (1985).

23) K. Lucke and K. Detert, Acta metall. 5, 628 (1957).

24) G. E. Dieter: " Mechanical Metallurgy", 2nd edition , Mcgraw-Hill Inc., 1976, p. 396.

25) E. M. Schulson, T. P. Weihs, D. V. Veins and I. Baker, Acta metall., 33, 1587 (1985).